8 Predicting the Thermodynamic Behavior of Water + Ionic Liquids Systems Using COSMO-RS

M. G. FREIRE
CICECO, Departamento de Química, Universidade de Aveiro, Aveiro, Portugal

L. M. N. B. F. SANTOS
CIQ, Departamento de Química, Faculdade de Ciências da Universidade do Porto, Porto, Portugal

I. M. MARRUCHO and J. A. P. COUTINHO
CICECO, Departamento de Química, Universidade de Aveiro, Aveiro, Portugal

Abstract

Ionic liquids are a novel class of chemical compounds with interesting properties that are driving much research in several fields. The complete understanding of the phase behavior of ionic liquids with water is an important issue, yet there is little data on their phase equilibria. In this work, the predictive capability of COSMO-RS, a predictive model based on unimolecular quantum chemistry calculations, was evaluated on the description of the liquid–liquid equilibria and the vapor–liquid equilibria of water and several imidazolium-based ionic liquid binary mixtures. The performance of the different calculation procedures, the basis set parameterizations, and the effect of the ion conformers on the quality of the predictions were evaluated. COSMO-RS calculations were performed at the following levels: BP/TZVP, BP/SVP//AM1, and B88-VWN/DNP. It was found that the calculation procedure based on the quantum chemical COSMO calculation at the BP/TZVP level derived from the lower energy ion conformations provides the best prediction capacity of the model. Good agreement between the model predictions and experimental VLE and LLE data was obtained. The COSMO-RS proved to be very helpful for scanning the growing set of already known ionic liquids in order to find suitable candidates for a certain task or to design new ionic liquids for specific applications.

Q1

Molten Salts and Ionic Liquids: Never the Twain? Edited by Marcelle Gaune-Escard and Kenneth R. Seddon

8.1 INTRODUCTION

Room-temperature ionic liquids are salts commonly composed of relatively large organic cations and inorganic or organic anions that cannot form an ordered crystal and thus remain liquid at or near room temperature. Unlike molecular liquids, the ionic nature of these liquids results in a unique combination of intrinsic physical properties such as high thermal stability, large liquidus range, high ionic conductivity, negligible vapor pressures, nonflammability, and a highly solvating capacity for both polar and nonpolar compounds. Among the several applications foreseeable for ionic liquids in the chemical industry, such as solvents in organic synthesis, as homogeneous and biphasic transfer catalysts, and in electrochemistry, there has been considerable interest in the potential of ionic liquids for separation processes as extraction media where, among others, ionic liquids have shown promise in the liquid–liquid extraction of organics from water [1–3]. Nevertheless, for the extraction of organic products from chemical reactions that proceed in aqueous media and for liquid–liquid extractions from aqueous phases, ionic liquids with lower solubility in water are preferred, and while they cannot contribute to air pollution due to their negligible vapor pressure, they do have in fact a significant solubility in water and, as a result, this is the most likely medium through which ionic liquids will enter the environment. Moreover, the loss of ionic liquids into the aqueous phase may be an important factor in estimating the cost of the ionic liquid used and the cost of water treatments. Furthermore, it was already shown that the presence of water in the ionic liquid phase can dramatically affect their physical properties [4, 5].

Another intrinsic attribute of ionic liquids is the potential of tuning their physical and chemical properties by varying different features of the ionic liquid, including the alkyl chain length and number of alkyl groups of the cation and the anion identity. At present, measurements on the solubility and phase equilibria of ionic liquids and water are limited. To our knowledge, only a few studies on these kinds of solubilities have been reported [6–12]. Thus, in our group, a systematic study of the liquid–liquid equilibria was conducted by variation of the cation chain length, in the presence of additional alkyl substitution on the cation, as well as in the anion identity. The main goal is to determine the impact of the different ionic liquids characteristics and the possibility to design a solvent for a specific application, in this case to fine-tune a particular ionic liquid with known mutual solubilities with water.

As it is infeasible to experimentally measure all possible combinations of anions and cations in ionic liquids vapor–liquid equilibria (VLE) and liquid–liquid equilibria (LLE) systems, it is essential to make measurements on selected systems to provide results that can be used to develop correlations and to test predictive methods. Several models have been used for correlating experimental data of phase equilibria with ionic liquids systems. Based on excess free Gibbs energy models, Wilson, UNIFAC, and UNIQUAC equations have been applied to correlate solid–liquid equilibria and VLE of ionic liquids [11, 13–16]. Another local composition model that proved capable of correlating data for ionic liquids systems was the nonrandom two-liquid (NRTL) model that was applied to VLE and LLE systems [16–19]. A different approach was proposed by Rebelo [20] that used a "polymer-like" G^E model to correlate the LLE of

ionic liquids solutions, because of the similarity between the LLE phase diagrams of polymer solutions and those of ionic liquid solutions. Nevertheless, correlations and group contribution methods are not a good alternative, due to the lack of experimental data at present. On the other hand, the use of equations of state (EoS) requires critical parameters of the ionic liquid, which are not directly measurable and have been obtained indirectly [21, 22]. However, on the basis of unimolecular quantum calculations of the individual molecules, the Conductor-like Screening Model for Real Solvents, COSMO-RS, appears to be a novel method for the prediction of thermophysical properties of fluids and can be considered as an alternative to the structure-interpolating group-contribution methods (GCMs) [23, 24]. The COSMO-RS is also based on a physically founded model but, unlike GCMs, uses only atom-specific parameters. This method is therefore, at least qualitatively, able to describe structural variations correctly. To our knowledge, two applications of COSMO-RS for ionic liquids LLE systems were found in the literature, concerning ionic liquids and alcohols, ethers or ketone systems [25, 26]. Conversely, no application of COSMO-RS to ionic liquid/water systems was previously attempted.

Thus the goal of the present study is to evaluate the COSMO-RS potential for prediction of the thermodynamic behavior for systems of ionic liquids and water for imidazolium-based ionic liquids, since no data for other family-based ionic liquids are currently available.

8.2 PHASE EQUILIBRIA PREDICTION OF SYSTEMS INVOLVING IONIC LIQUIDS AND WATER

Traditional approaches for correlating or predicting the properties of fluid mixtures such as EoS methods and schemes based primarily on dividing the molecules into various groups (GCMs) require a large bank of experimental data prior to their application. At present, the major requirement is a predictive method that could screen the huge number of possible combinations of ionic liquids and their mixtures, in this study with water, prior to making extensive experimental measurements.

The COSMO-RS is a unique method for predicting the thermodynamic properties of mixtures on the basis of unimolecular quantum chemical calculations for the individual molecules [23–27]. COSMO-RS combines the electrostatic advantages and the computational efficiency of the quantum chemical dielectric continuum solvation model COSMO with a statistical thermodynamics approach, based on the results of the quantum chemical calculations [28, 29]. The standard procedure of COSMO-RS calculations consists of two steps: quantum chemical COSMO calculations for all the molecular species involved, and COSMO-RS calculations [28, 29].

The quantum chemical model COSMO is an efficient variant of dielectric continuum solvation methods. In these calculations, the solute molecules are assumed to be in a virtual conductor environment, where the solute molecule induces a polarization charge density σ on the interface between the molecule and the conductor, that is, on the molecular surface. These charges act back on the solute and generate a more polarized electron density than in a vacuum. During the quantum

chemical self-consistency cycle, the solute molecule is thus converged to its energetically optimal state in a conductor with respect to electron density, and the molecular geometry can be optimized using conventional methods for calculations in a vacuum. Although time consuming, one advantage of this procedure is that the quantum chemical calculations have to be performed just once for each molecule of interest.

The COSMO-RS calculation procedure, performed using the COSMOtherm program [28, 29], describes all the interactions between molecules as contact interactions of the molecular surfaces, and these interactions can be related to the screening charge densities σ and σ' of the interacting surface pieces. For the statistical mechanical calculation, the molecular surface is split into small effective areas, a_{eff}, and contact with each of these areas is considered to be independent. The difference between the two screening charge densities of a particular pair causes a specific interaction energy that, in combination with the energy contributions of hydrogen bonds and the van der Waals interactions, allows the interactions of the components of a particular mixture to be determined. The application of statistical thermodynamics gives the chemical potential of each component, and from these LLE, VLE, and other properties of any mixture are derived. It should be noted that these calculations do not depend on any properties of the ionic liquids mixtures. Furthermore, the mixture properties are calculated from an entropy term based on the surface area and volume of the molecules, and an enthalpy term that is calculated from the energies of interaction between the surfaces of the molecules.

Within the COSMOtherm program, a *pseudo-binary* approach was used to calculate the LLE and VLE of a mixture composed of an ionic liquid and water, with the cation and anion of the ionic liquid input as separate compounds with the same mole fraction. The chemical potentials are calculated for the ternary system (anion + cation + water) with the chemical potential of the ionic liquid as the sum of the chemical potentials of both the cation and anion. For the case of LLE, a numerical approach is used to find the two compositions having equal chemical potentials of the three components (in the pseudo-binary system) in the two phases at a particular temperature.

In order to evaluate the performance of the different calculation procedures and basis set parameterizations on the quality of the predictions, COSMO-RS calculations were done at the following levels:

- BP/TZVP (Turbomole [30], DFT/COSMO calculation with the BP functional and TZVT [31] basis set using the optimized geometries at the same level of theory)—parameter file: BP_TZVP_C21_0105.
- BP/SVP/AM1 (Turbomole [30], DFT/COSMO single-point calculation with the BP functional and SVT [31] basis set upon geometries optimized at semiempirical MOPAC-AM1/COSMO level)—parameter file: BP_SVP_AM1_C21_0105.
- B88-VWN/DNP (DMOL3 [32], DFT/COSMO calculation with the B88-VWN functional and numerical DNP [32] basis using the optimized geometries at the same level of theory)—parameter file: DMOL3_C21_0105.

8.3 LLE AND VLE EXPERIMENTAL DATABASE

Liquid–liquid equilibria experimental measurements between water and imidazolium-based ionic liquids were studied for the following ionic liquids: 1-butyl-3-methylimidazolium hexafluorophosphate ($[C_4mim][PF_6]$), 1-butyl-3-hexylimidazolium hexafluorophosphate ($[C_6mim][PF_6]$), 1-octyl-3-methylimidazolium hexafluorophosphate ($[C_8mim][PF_6]$), 1-butyl-2,3-dimethylimidazolium hexafluorophosphate ($[C_4C_1mim][PF_6]$), 1-ethyl-3-methylimidazolium bis(trifluoromethylsulfonyl)amide ($[C_2mim][NTf_2]$), 1-butyl-3-methylimidazolium bis(trifluoromethylsulfonyl)amide ($[C_4mim][NTf_2]$), 1-hexyl-3-methylimidazolium bis(trifluoromethylsulfonyl)amide ($[C_6mim][NTf_2]$), 1-heptyl-3-methylimidazolium bis(trifluoromethylsulfonyl)amide ($[C_7mim][NTf_2]$), 1-octyl-3-methylimidazolium bis(trifluoromethylsulfonyl)amide ($[C_8mim][NTf_2]$), and 1-octyl-3-methylimidazolium tetrafluoroborate ($[C_8mim][BF_4]$). The ionic liquid content in the water-rich phase was analyzed using UV-Vis spectroscopy, and the water content in the ionic liquid-rich phase was analyzed by Karl Fischer titration. The temperature range of the experimental analysis was between 288 and 318 K and at atmospheric pressure. Further details about the experimental procedure and respective results can be found elsewhere [33, 34].

Vapor–liquid equilibria experimental isothermal measurements between water and imidazolium-based ionic liquids were taken from Anthony et al. [6] for $[C_4mim][PF_6]$, $[C_8mim][PF_6]$, and $[C_4mim][BF_4]$ and from Kato and Gmehling [11] for $[C_2mim][NTf_2]$, $[C_4mim][NTf_2]$, and 1-methyl-3-methylimidazolium dimethylphosphate ($[C_1mim][(CH_3)_2PO_4]$).

8.4 RESULTS AND DISCUSSION

Prior to extensive comparisons between COSMO-RS predictions and the experimental data available, some studies concerning the COSMO-RS calculations were carried out. Different calculation procedures, basis set parameterizations, and the use of different energy conformers were evaluated to assess the performance of the predictive results. After defining the best conditions for the COSMO-RS procedure, comparisons between modeling results and experimental data were conducted. The effect of the alkyl chain length, methyl inclusion, anion identity, and temperature dependence in both LLE and VLE systems are presented and discussed.

8.5 PARAMETERIZATION INFLUENCE ON THE PREDICTIONS

The quality, accuracy, and systematic errors of the electrostatic energies resulting from the underlying quantum chemical calculations depend on the quantum chemical method as well as on the basis set/parameterization combinations. For that reason, three parameterizations coupled with the COSMOtherm program were tested, both on the LLE and VLE predictions using different calculation procedures and basis set

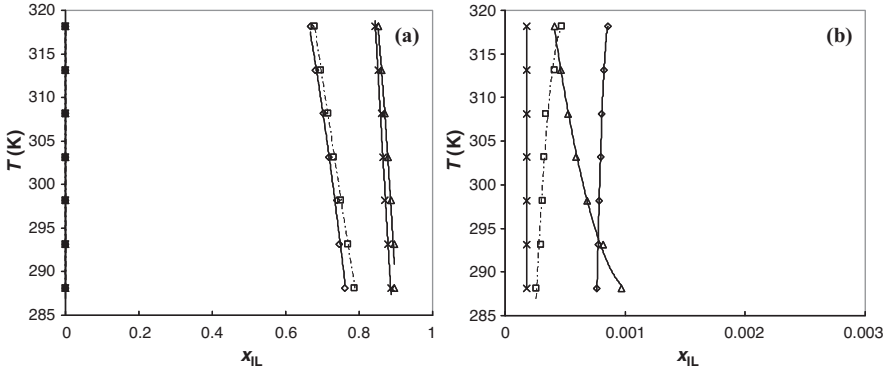

FIGURE 8.1 Liquid–liquid phase diagram for water and $[C_4mim][Tf_2N]$: □, experimental; ◊, BP/TZVP; Δ, BP/SVP//AM1; ×, B88-VWN/DNP. The dashed and the solid lines represent, respectively, the experimental data and the prediction by the COSMO-RS calculation.

parameterizations: namely; BP/TZVP, BP/SVP//AM1, and B88-VWN/DNP, as described previously. The calculations for the three parameterizations tested were performed with the minimum energy conformers for one LLE example and one VLE example, and the results are presented in Figures 8.1 and 8.2.

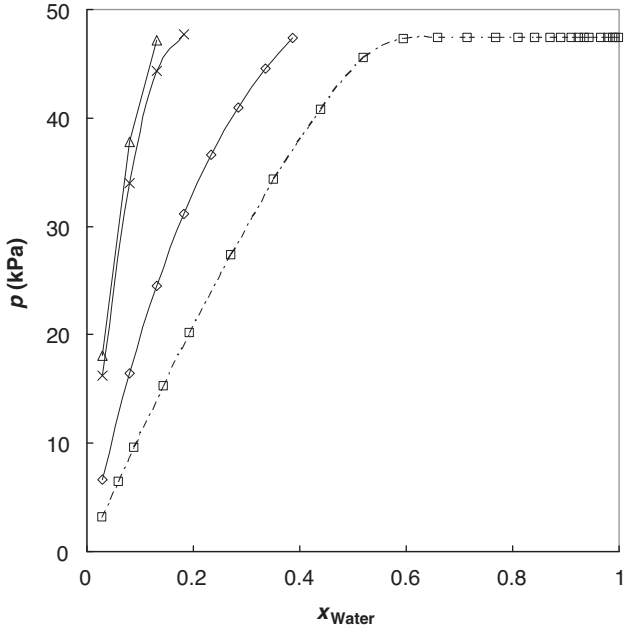

FIGURE 8.2 Vapor–liquid phase diagram for water and $[C_2mim][Tf_2N]$: □, experimental; ◊, BP/TZVP; Δ, BP/SVP//AM1; ×, B88-VWN/DNP. The dashed and the solid lines represent, respectively, the experimental data and the prediction by the COSMO-RS calculation.

The question of which quantum chemistry method and basis set and also which parameterization of COSMOtherm to use for an application depends on the required quality and the later usage of the predictions. The results obtained here show, in accordance with the suggestions of Eckert [29], that the BP/TZVP procedure is the best choice because it is the result of a high-quality quantum chemistry method in combination with a large basis set and therefore is able to capture the strong polarity of ionic species. In fact, for the LLE and VLE prediction of the binary mixtures, in general, the best results in description of the experimental data were achieved with the BP/TZVP procedure.

8.6 CONFORMERS INFLUENCE ON THE PREDICTIONS

A molecule prefers to occupy the levels of the minimum potential energy and arranges its atoms accordingly. By rotation around single bonds, molecules with the same molecular formula can form geometrical isomers by arranging their atoms in different, nonequivalent positions to each other, the so-called minimum energy conformations or stable conformations. There are different energy states for the various conformers in the alkyl chains of $[C_2mim]^+$ to $[C_8mim]^+$ cations and in the $[NTf_2]^-$ and $[(CH_3)_2PO_4]^-$ anions studied. Thus it is important from a theoretical point of view to evaluate the effect of the various conformers on the predicted LLE and VLE systems. To study the influence of the ionic liquids conformations on the COSMO-RS predictions, the stable conformations with the minimum and the maximum COSMO energy have been tested. The minimum energy conformations of the ionic liquids consist of the geometrically optimized minimum energy structure of the cation and the anion and the maximum energy conformations consist of the opposite analogy; besides the $[NTf_2]^-$ and $[(CH_3)_2PO_4]^-$ anions that were found to have two and three stable conformers each, in some cases just the effect of the cation is studied, because only one structure of the anions $[PF_6]^-$ and $[BF_4]^-$ exists. Some examples of the conformer influence results are depicted in Figures 8.3–8.5, both in the LLE and VLE phase diagrams.

The results presented in Figure 8.3 show that the different cation energy conformations have a small effect on the predicted mutual solubilities, and similar behaviors in the LLE study for other alkyl chain length examples and also in combination with the $[BF_4]^-$ anion were obtained. Higher deviations were found in the $[C_4mim][NTf_2]$ ionic liquid phase diagram presented in Figure 8.4, where besides the presence of the cation conformers, the anion also presents two different minimum energy geometrical isomers. There is a combination of minimal energy conformations of both cation and anion, showing that the anion plays an important role in the interactions with water. The $[NTf_2]^-$ anion has four atoms of oxygen and the interaction between these and hydrogen from water will be stronger and hydrogen bonded, compared to the $[BF_4]^-$ and $[PF_6]^-$ anions.

One example of the diverse energy conformations influence on the VLE behavior is presented in Figure 8.5. In both cases of the $[C_2mim][NTf_2]$ and $[C_4mim][NTf_2]$ with

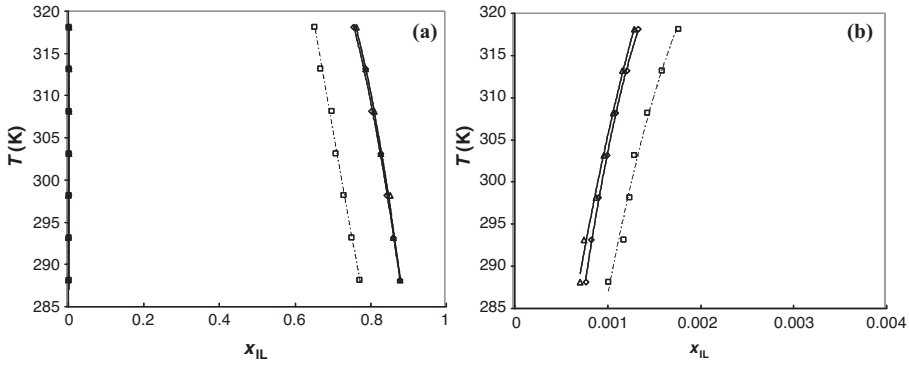

FIGURE 8.3 Complete liquid–liquid phase diagrams for (a) water and [C_4mim][PF_6] and (b) in the water–rich phase: □, experimental; ◊, lower energy conformation; Δ, higher energy conformation. The dashed and the solid lines represent, respectively, the experimental data and the prediction by the COSMO-RS calculation using the BP/TZVP procedure.

water vapor–liquid phase diagrams, the positive deviation from Raoult's law is predicted, and the best results with respect to experimental data are that with ions of lower energy conformation.

In general, the LLE of systems with imidazolium-based ionic liquids and water seem to be more affected by the presence of the different conformers of the anion than the VLE phase diagram, where the higher deviations were found with the cation multiple conformations.

In both the LLE and VLE studies, the best predictions were obtained with the lower energy conformations of both cation and/or anion.

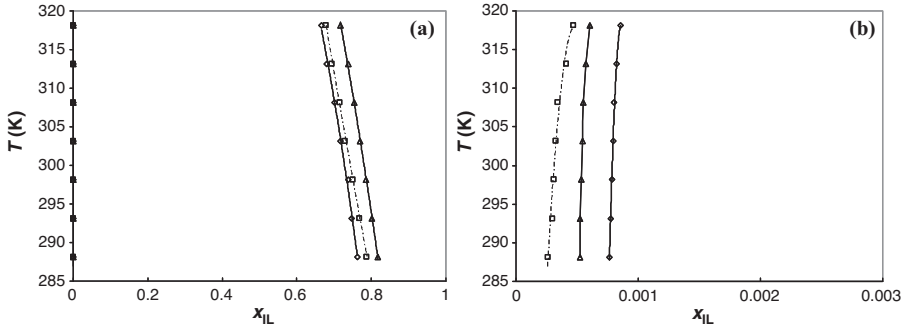

FIGURE 8.4 Complete liquid–liquid phase diagrams for (a) water and [C_4mim][NTf_2] and (b) in the water-rich phase: □, experimental; ◊, lower energy conformation; Δ, higher energy conformation. The dashed and the solid lines represent, respectively, the experimental data and the prediction by the COSMO-RS calculation using the BP/TZVP procedure.

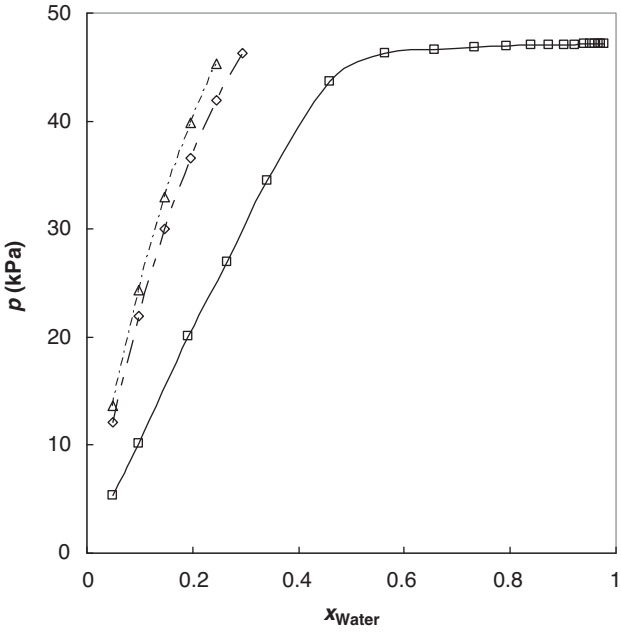

FIGURE 8.5 Vapor–liquid phase diagram for water and $[C_4mim][NTf_2]$: □, experimental; ◊, lower energy conformation; Δ, higher energy conformation. The dashed and the solid lines represent, respectively, the experimental data and the prediction by the COSMO-RS calculation using the BP/TZVP procedure.

8.7 LIQUID–LIQUID EQUILIBRIA MODELING

Having established the best parameterization and the optimal conformers, the phase diagram for a number of binary ionic liquid–water systems was predicted. In this part of the work, the quantum chemical COSMO calculations for the ionic liquids under study were performed with the Turbomole program package [30] using the BP density functional theory and the triple-ζ valence polarized large basis set (TZVP) [31]. These calculations were made for a true three-component mixture, where the cation and anion of equal concentrations are treated as separate species, and were performed with the optimized minimum energy conformations of both the cation and/or the anion. Experimental data in the form of T–x data for each binary mixture investigated and the results obtained with the COSMO-RS calculations are compared in Figures 8.6–8.10.

Q2

The ionic liquids–water systems studied presented an asymmetric LLE behavior due to the high solubility of water in ionic liquids while their solubility in water is very limited, ranging from 10^{-5} to 10^{-2} mol·L^{-1}. Imidazolium-based ionic liquids can act as both hydrogen bond acceptors (anion) and donors (cation) and would be expected to interact with solvents with both accepting and donating sites, such as water. Water is

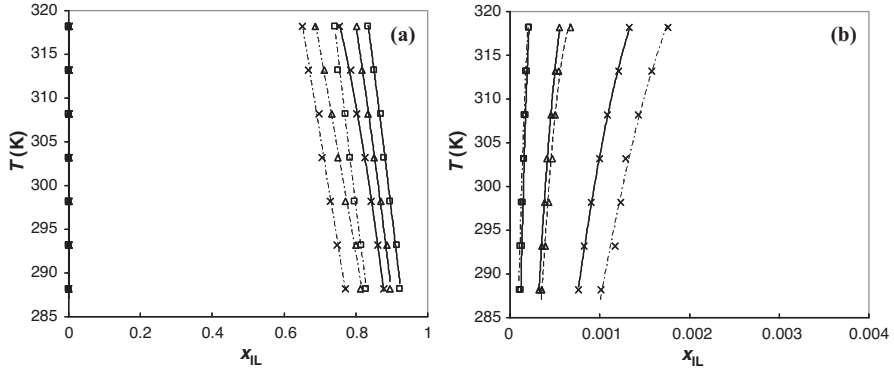

FIGURE 8.6 Comparison of the liquid–liquid phase diagrams for (a) water and ionic liquids and (b) the water-rich phase: ×, [C_4mim][PF_6]; Δ, [C_6mim][PF_6]; □, [C_8mim][PF_6]. The dashed and the solid lines represent, respectively, the experimental data and the prediction by the COSMO-RS calculation using the BP/TZVP procedure.

well known to form hydrogen-bonded networks with both high enthalpies and constants of association, and it is expected to stabilize with hydrogen-bond donor sites. However, the existence of the liquid–liquid phase equilibria in these mixtures is the evidence that the interaction between the ionic liquid and water is not very significant, and that the ion–ion and water–water interactions were stronger than water–ion interactions in the observed mixtures.

The results obtained are discussed below from different perspectives to evaluate the impact of the ionic liquids structural variations and the COSMO-RS predictive capability for mutual solubilities.

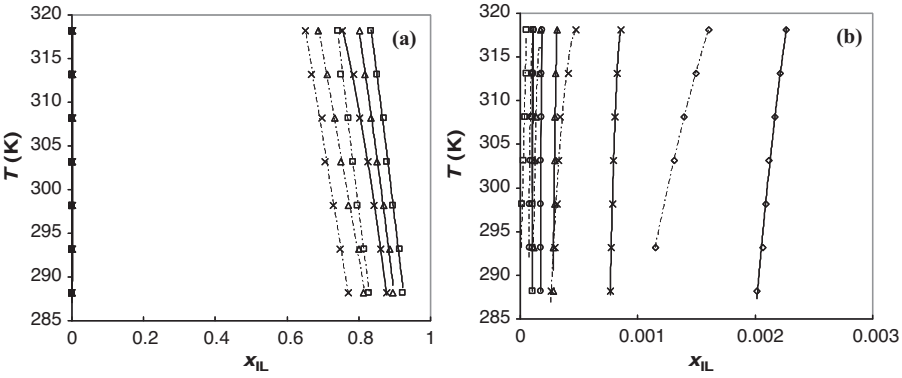

FIGURE 8.7 Comparison of the liquid–liquid phase diagrams for (a) water and ionic liquids and (b) the water-rich phase: ◊, [C_2mim][NTf_2]; ×, [C_4mim][NTf_2]; Δ, [C_6mim][NTf_2]; ○, [C_7mim][NTf_2]; □, [C_8mim][NTf_2]. The dashed and the solid lines represent, respectively, the experimental data and the prediction by the COSMO-RS calculation using the BP/TZVP procedure.

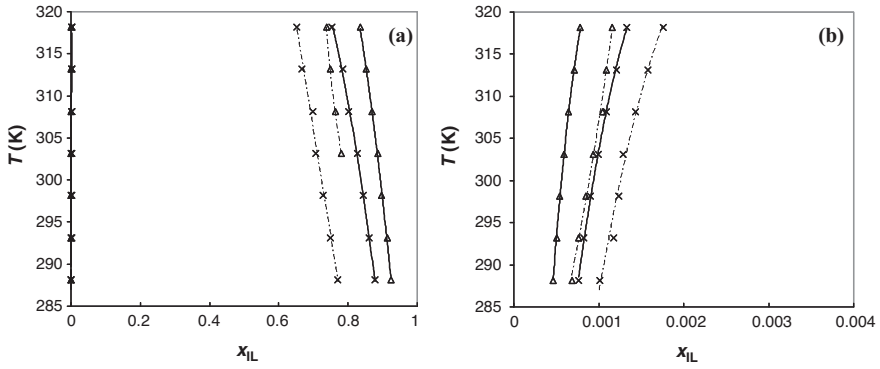

FIGURE 8.8 Comparison of the liquid–liquid phase diagrams for (a) water and ionic liquids and (b) the water-rich phase: ×, [C_4mim][PF_6]; Δ, [C_4C_1mim][PF_6]. The dashed and the solid lines represent, respectively, the experimental data and the prediction by the COSMO-RS calculation using the BP/TZVP procedure.

8.7.1 Cation Alkyl Chain Length

Figures 8.6 and 8.7 show the liquid–liquid phase behavior for two anions, $[PF_6]^-$ and $[NTf_2]^-$, in combination with different alkyl chain length imidazolium-based ionic liquids. Due to the asymmetrical character of the LLE behavior, the figures present both the general LLE diagrams and the water-rich side of the equilibrium.

The influence of the cation alkyl chain length in the mutual solubilities was verified to follow the same trend with both the anions, where there is a hydrophobicity increase concomitant with the cation alkyl chain length increase. That hydrophobic tendency occurs at both sides of the equilibrium, but plays a major role on the water-rich side,

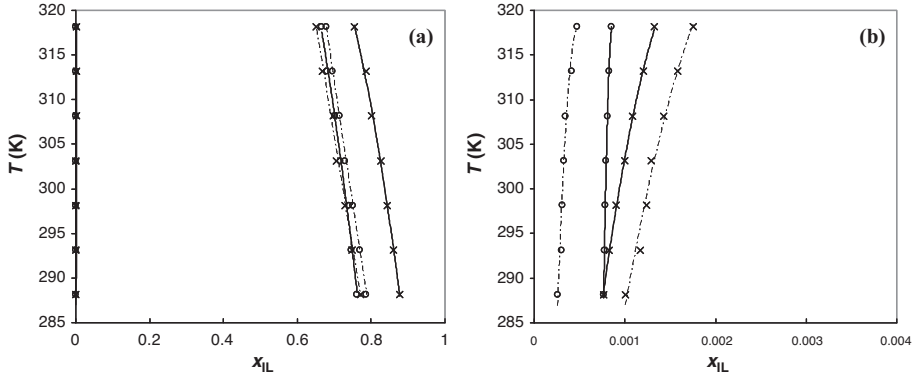

FIGURE 8.9 Comparison of the liquid–liquid phase diagrams for (a) water and ionic liquids and (b) the water-rich phase: ◯, [C_4mim][NTf_2]; ×, [C_4mim][PF_6]. The dashed and the solid lines represent, respectively, the experimental data and the prediction by the COSMO-RS calculation using the BP/TZVP procedure.

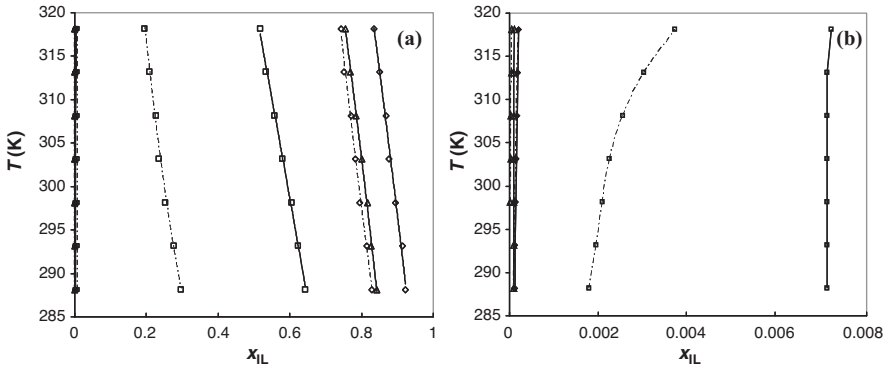

FIGURE 8.10 Comparison of the liquid–liquid phase diagrams for (a) water and ionic liquids and (b) the water-rich phase: Δ, [C_8mim][NTf_2]; ◊, [C_8mim][PF_6]; □ [C_8mim][BF_4]. The dashed and the solid lines represent, respectively, the experimental data and the prediction by the COSMO-RS calculation using the BP/TZVP procedure.

where differences of one order of magnitude appear when comparing the solubility of [C_4mim][PF_6] with [C_8mim][PF_6], and even of two orders of magnitude when comparing [C_2mim][NTf_2] with [C_8mim][NTf_2] in water.

The results obtained from COSMO-RS calculations show an acceptable agreement with the experimental data available, and follow the same hydrophobicity tendency to increase with the cation alkyl chain length increase, depicting the qualitatively good prediction capacity of this model. Higher relative deviations were found in the water-rich phase, but it should be mentioned that there is a relatively low solubility of ionic liquids in water, and the predictions were always of the same order of magnitude as the experimental data; that is, if the solubilities were reported as $\log(x)$, as is usual in this field, the difference between the experimental data and the predictions is well below one log unit.

8.7.2 Cation Methyl Inclusion

Figure 8.8 presents the comparison between water and [C_4mim][PF_6] or [C_4C_1mim][PF_6] mutual solubilities.

By replacing the hydrogen of the [C_4mim]$^+$ cation at the C2 position with a methyl group (forming [C_4C_1mim]$^+$), the ability of the cation to hydrogen bond with water is greatly diminished, resulting in a decrease in the mutual solubilities between the previous imidazolium-based ionic liquid and water. Clearly, hydrogen bonding of water with the acidic hydrogen of the imidazolium cation has some influence in controlling liquid–liquid phase behavior between imidazolium-based ionic liquids and water. COSMO-RS calculations agree well with experimental results for both sides of the equilibrium, predicting correctly the increased hydrophobicity and the variation in mutual solubilities due to a methyl inclusion in the imidazolium cation.

8.7.3 Anion Identity

Figures 8.9 and 8.10 show the comparison between the experimental data and COSMO-RS predictions using the BP/TZVP procedure for the liquid–liquid phase behavior for two independent cations, $[C_4mim]^+$ and $[C_8mim]^+$, in combination with different anions, $[NTf_2]^-$, $[PF_6]^-$, and $[BF_4]^-$.

An excellent predictive capacity was found for the case of the $[C_4mim][NTf_2]$ entire liquid–liquid phase diagram. Also, in the water-rich phase, COSMO-RS proved to predict the hydrophobic tendency increase due to the anion identity from $[BF_4]^- < [PF_6]^- < [NTf_2]^-$, following the experimental mutual solubilities decrease with water. However, from Figure 8.9, in the ionic liquid-rich phase, the hydrophobic tendency between $[PF_6]^-$ and $[NTf_2]^-$ is not well described when compared to the experimental data. COSMO-RS predicts a higher solubility of water in $[C_4mim][NTf_2]$ than in $[C_4mim][PF_6]$, which may be due to the fact that $[NTf_2]^-$ is a stronger Lewis base than $[PF_6]^-$. Conversely, $[PF_6]^-$ has a greater charge density than $[NTf_2]^-$ because it is smaller, so it can have stronger Coulombic interactions, and clearly the phase behavior is the result of several competing interactions in the solution.

Moreover, it was demonstrated that both the cation and anion affect the mutual solubilities, but from Figures 8.9 and 8.10, it is the anion that plays the major role on the phase behavior of imidazolium-based ionic liquids with water. Thus changing the anion is the easiest way to adjust the liquid–liquid equilibrium with water.

8.8 VAPOR–LIQUID EQUILIBRIA MODELING

The vapor-phase behavior for six ionic liquid–water systems was available from the literature [6, 11] and the comparison of the COSMO-RS predictions, using the BP/TZVP procedure and the lower energy ion conformations, with the experimental data was performed. The results are presented in Figures 8.11–8.14 in the form of p–x data for each binary mixture investigated. Again, the COSMO-RS calculations were made for a true three-component mixture where the cation and anion of equal concentrations are treated as separate species. The results obtained for the isotherm p–x phase diagrams are discussed below from different views to evaluate the influence of the ionic liquids structural variations and their dependence on temperature and the COSMO-RS predictive capability.

8.8.1 Cation Alkyl Chain Length

Figures 8.11 and 8.12 show the vapor–liquid phase behavior for two anions, $[PF_6]^-$ and $[NTf_2]^-$, in combination with different alkyl chain length imidazolium-based ionic liquids.

From Figures 8.11 and 8.12, COSMO-RS provided a good description of the p–x phase diagrams with respect to the cation alkyl chain length variation with both the anions, $[PF_6]^-$ and $[NTf_2]^-$, when compared to the experimental data [6, 11]. There is an increase of the positive deviation from Raoult's law and an increase of the ionic

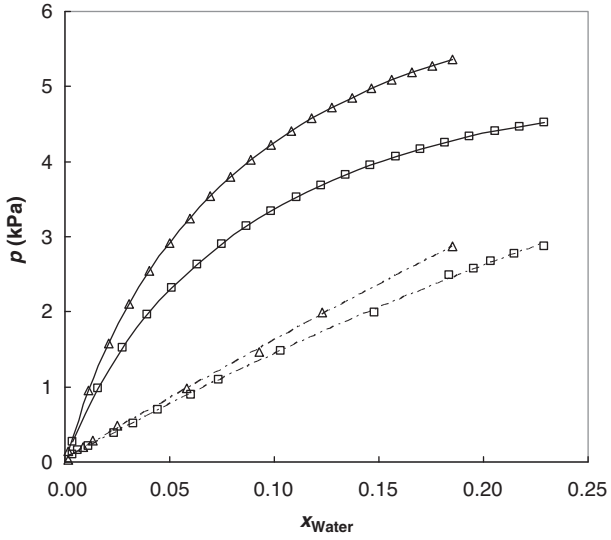

FIGURE 8.11 Comparison of the vapor–liquid phase diagrams for water and ionic liquids at 298.15 K: □, [C_4mim][PF_6]; Δ, [C_8mim][PF_6]. The dashed and the solid lines represent, respectively, the experimental data [6] and the prediction by the COSMO-RS calculation using the BP/TZVP procedure.

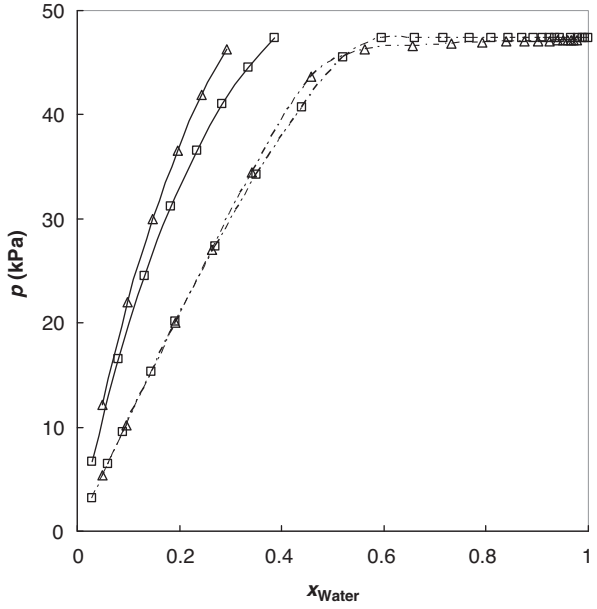

FIGURE 8.12 Comparison of the vapor–liquid phase diagrams for water and ionic liquids at 353.15 K: □, [C_2mim][NTf_2]; Δ, [C_4mim][NTf_2]. The dashed and the solid lines represent, respectively, the experimental data [11] and the prediction by the COSMO-RS calculation using the BP/TZVP procedure.

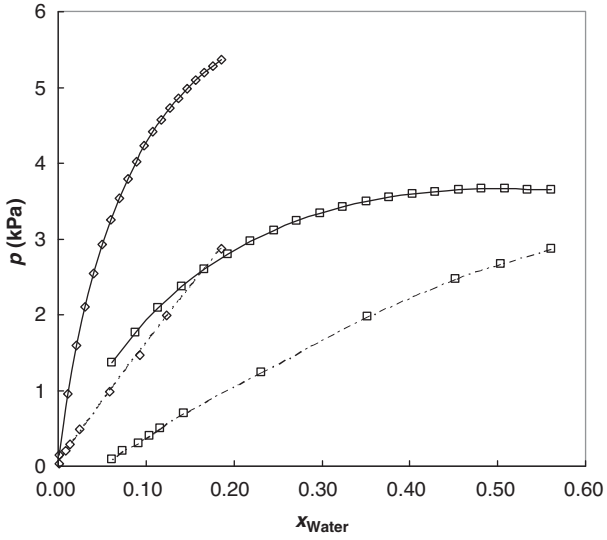

FIGURE 8.13 Comparison of the vapor–liquid phase diagrams for water and ionic liquids at 298.15 K: ◊, $[C_8mim][PF_6]$; □, $[C_8mim][BF_4]$. The dashed and the solid lines represent, respectively, the experimental data [6] and the prediction by the COSMO-RS calculation using the BP/TZVP procedure.

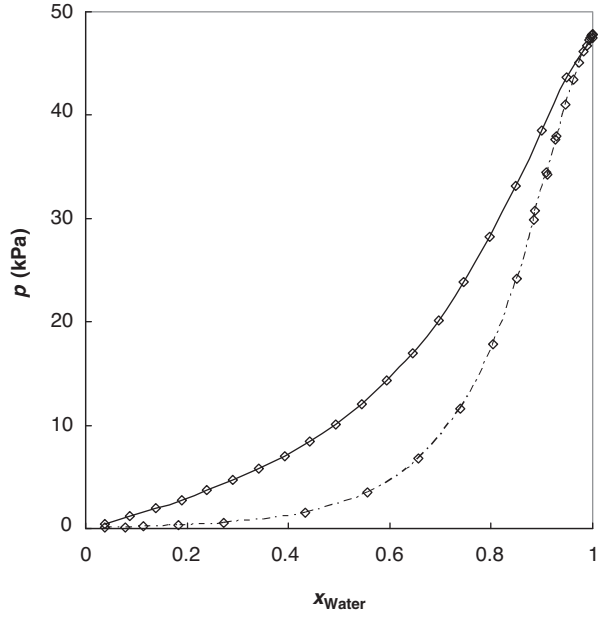

FIGURE 8.14 Comparison of the vapor–liquid phase diagrams for water and $[C_1mim][(CH_3)_2PO_4]$ at 353.15 K. The dashed and the solid lines represent, respectively, the experimental data [6] and the prediction by the COSMO-RS calculation using the BP/TZVP procedure.

liquids' hydrophobicity with the alkyl chain length increase. In Figure 8.12 the occurrence of a miscibility gap with the $[NTf_2]^-$ based ionic liquids is shown; this same behavior is expected with the $[PF_6]^-$ based ionic liquids, although the mole fraction range presented is not enough to prove this fact experimentally. Besides the positive deviation from Raoult's law that is predicted for the ionic liquids based on these two anions, COSMO-RS was able to give at least a priori good qualitative predictions.

8.8.2 Anion Identity

Figure 8.13 shows the comparison between experimental data [6] and COSMO-RS predictions using the BP/TZVP procedure for the vapor–liquid phase behavior for the $[C_8mim]^+$ cation, in combination with different anions $[NTf_2]^-$ and $[PF_6]^-$. Figure 8.14 presents the results obtained for water with the $[C_1mim][(CH_3)_2PO_4]$ ionic liquid vapor–liquid phase equilibria [11].

COSMO-RS proved to predict the hydrophobic tendency increase in the vapor–-liquid phase equilibria due to the anion identity from $[BF_4]^- < [PF_6]^-$, following the same trend of the liquid–liquid equilibria.

Moreover, it was demonstrated that both the cation and anion affect the vapor–liquid phase equilibria but, comparing Figures 8.11–8.13, it is the anion that plays the major role in the vapor-phase behavior of imidazolium-based ionic liquids with water, as in the LLE systems.

From Figure 8.14, COSMO-RS demonstrated that it is also able to describe phase diagrams with strong negative deviations from Raoult's law, as experimentally evidenced.

8.8.3 Temperature Dependence

Figures 8.15–8.17 show the comparison between the experimental data [6] and COSMO-RS predictions using the BP/TZVP procedure for the vapor–liquid phase behavior at several isotherms for the following ionic liquids: $[C_4mim][PF_6]$, $[C_8mim][PF_6]$, and $[C_8mim][BF_4]$.

From Figures 8.15–8.17, COSMO-RS showed the ability to describe the vapor–-liquid phase diagram behavior as a function of temperature, increasing pressure with the increase of temperature, as verified experimentally. Although the quantitative predictions are not so excellent, COSMO-RS was able to describe the qualitative variations due to temperature in all the ionic liquids analyzed which were composed of different cations and/or anions.

8.9 CONCLUSION

Ionic liquids have been suggested as potential "green" solvents to replace volatile organic solvents in reaction and separation processes due to their negligible vapor pressure. To develop ionic liquids for these applications, it is important to gain a

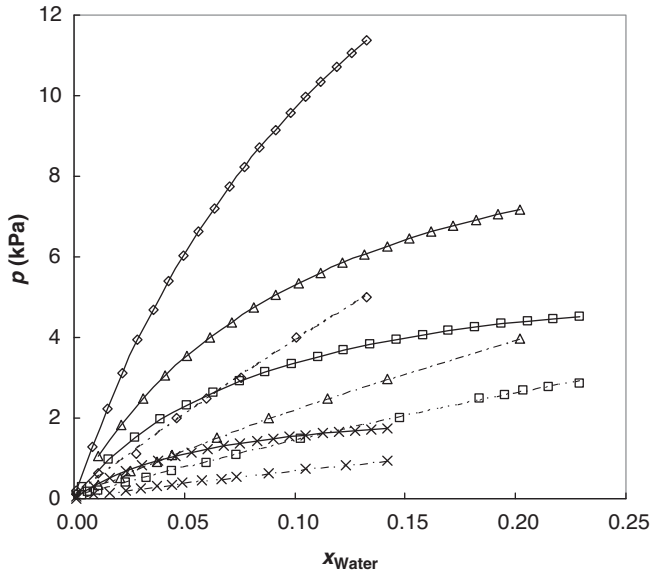

FIGURE 8.15 Comparison of the vapor-liquid phase diagrams for water and $[C_4mim][PF_6]$ at isotherms: ×, 283.15 K; □, 298.15 K; Δ, 308.15 K; ◊, 323.15 K. The dashed and the solid lines represent, respectively, the experimental data and the prediction by the COSMO-RS calculation.

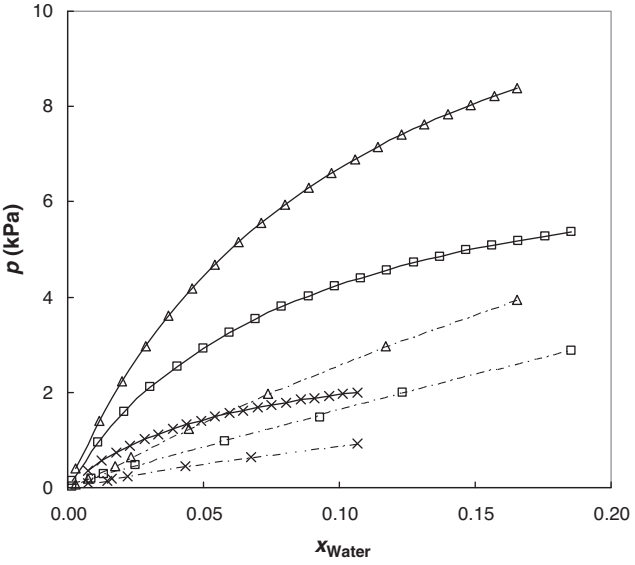

FIGURE 8.16 Comparison of the vapor–liquid phase diagrams for water and $[C_8mim][PF_6]$ at isotherms: ×, 283.15 K; □, 298.15 K; Δ, 308.15 K. The dashed and the solid lines represent, respectively, the experimental data and the prediction by the COSMO-RS calculation.

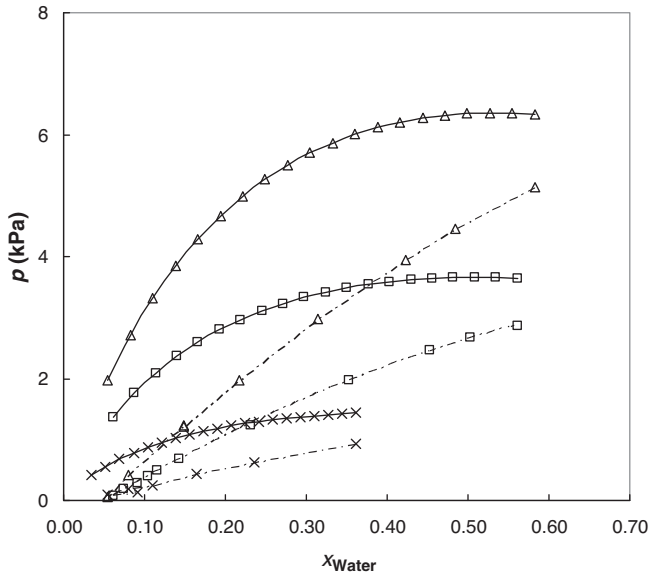

FIGURE 8.17 Comparison of the vapor–liquid phase diagrams for water and $[C_8mim][BF_4]$ at isotherms: ×, 283.15 K; □, 298.15 K; Δ, 308.15 K. The dashed and the solid lines represent, respectively, the experimental data and the prediction by the COSMO-RS calculation.

fundamental understanding of the factors that control the phase behavior of ionic liquids with other liquids, including polar solvents such as water. Since it is not feasible to experimentally determine all possible combinations with ionic liquids, a predictive method capable of describing the phase behavior of such systems is extremely important. Quantum chemical calculations based on the σ profiles of the cation, the anion, and water were used for the prediction of LLE and VLE systems incorporating ionic liquids and water. COSMO-RS and its implementation in the program COSMOtherm was shown to be capable of giving satisfactory a priori predictions of the thermodynamics of systems involving ionic liquids, which may be of considerable value for the exploration of suitable ionic liquids for practical and specific applications.

ACKNOWLEDGMENTS

The authors acknowledge financial support from Fundação para a Ciência e a Tecnologia (Project POCI/EQU/58152/2004) and a Ph.D. grant (SFRH/BD/14134/2003) to Mara G. Freire. They also acknowledge F. Eckert and A. Klamt, COSMOtherm, Version C2.1, Release 01.05, COSMOlogic GmbH & Co. KG, Leverkusen, Germany, 2005, and M. Diedenhofen of COSMOlogic for advice and assistance in the use of COSMOtherm.

REFERENCES

1. Huddleston, J. G., Willauer, H. D., Swatloski, R. P., Visser, A. E., and Rogers, R. D., Room temperature ionic liquids as novel media for clean liquid-liquid extraction, *Chem. Commun.* **44**, 1765–1766 (1998).
2. Fadeev, A. G. and Meagher, M. M., Opportunities for ionic liquids in recovery of biofuels, *Chem. Commun.* **44**, 295–296 (2001).
3. McFarlane, J., Ridenour, W. B., Luo, H., Hunt, R. D., DePaoli, D. W., and Ren, R. X., Room temperature ionic liquids for separating organics from produced water, *Sep. Sci. Technol.* **40**, 1245–1265 (2005).
4. Seddon, K. R., Stark, A., and Torres, M.-J., Influence of chloride, water, and organic solvents on the physical properties of ionic liquids, *Pure Appl. Chem.* **72**, 2275–2287 (2000).
5. Huddleston, J. G., Visser, A. E., Reichert, W. M., Willauer H. D., Broker, G. A., and Rogers, R. D., Characterisation and comparison of hydrophilic and hydrophobic room temperature ionic liquids incorporating the imidazolium cation, *Green Chem.* **3**, 156–164 (2001).
6. Anthony, J. L., Maggin, E. J., and Brennecke J. F., Solution thermodynamics of imidazolium-based ionic liquids and water, *J. Phys. Chem. B* **105**, 10942–10949 (2001).
7. Wong, D. S. H., Chen, J. P., Chang, J. M., and Chou, C. H., Phase equilibria of water and ionic liquids [emim][PF_6] and [bmim]PF_6], *Fluid Phase Equilib.* **194–197**, 1089–1095 (2002).
8. Crosthwaite, J. M., Aki, S. N. V. K., Maggin, E. J., and Brennecke, J. F., Liquid phase behavior of imidazolium-based ionic liquids with alcohols, *J. Phys. Chem. B* **108**, 5113–5119 (2004).
9. Rebelo, L. P. N., Najdanovic-Visak, V., Visak, Z. P., Nunes da Ponte, M., Szydlowski, J., Cerdeiriña, C. A., Troncoso, J., Romaní, L., Esperan a, J. M. S. S., Guedes, H. J. R., and de Sousa, H. C., A detailed thermodynamic analysis of [C_4mim][BF_4] + water as a case study to model ionic liquid aqueous solutions, *Green Chem.* **6**, 369–381 (2004).
10. Najdanovic-Visak, V., Esperan a, J. M. S. S., Rebelo, L. P. N., Nunes da Ponte, M., Guedes, H. J. R., Seddon, K. R., and Szydlowskiy, J., Phase behaviour of room temperature ionic liquid solutions: an unusually large co-solvent effect in (water + ethanol), *Phys. Chem. Chem. Phys.* **4**, 1701–1703 (2002).
11. Kato, R. and Gmehling, J., Measurement and correlation of vapour–liquid equilibria of binary systems containing the ionic liquids [EMIM][$(CF_3SO_2)_2N$], [MMIM][$(CF_3SO_2)_2N$], [MMIM][$(CH_3)_2PO_4$] and oxygenated organic compounds respectively water, *Fluid Phase Equilib.* **231**, 38–43 (2005).
12. Calvar, N., González, B., Gómez, E., and Domínguez, A., Vapor–liquid equilibria for the ternary system ethanol + water + 1-butyl-3-methylimidazolium chloride and the corresponding binary systems at 101.3 kPa, *J. Chem. Eng. Data* **51**, 2178–2181 (2006).
13. Domańska, U., Bogel-Łukasik, E., and Bogel-Łukasik, R., 1-Octanol/water coefficients of 1-alkyl-3-methyllimidazolium chloride, *Chem. Eur. J.* **9**, 3033–3041 (2003).
14. Domańska, U., Thermophysical properties and thermodynamic phase behavior of ionic liquids, *Thermochim. Acta* **448**, 19–30 (2006).
15. Domańska, U. and Bogel-Łukasik, E., Measurements and correlation of the (solid + liquid) equilibria of [1-decyl-3-methylimidazolium chloride + alcohols (C2–C12), *Ind. Eng. Chem. Res.* **42**, 6986–6992 (2003).

16. Doker, M. and Gmehling, J., Measurement and prediction of vapor–liquid equilibria of ternary systems containing ionic liquids, *Fluid Phase Equilib*. **227**, 255–266, (2005).
17. Hu, X., Yu, J., and Liu, H., Liquid–liquid equilibria of the system 1-(2-hydroxyethyl)-3-methylimidazolium tetrafluoroborate or 1-(2-hydroxyethyl)-2,3-dimethylimidazolium tetrafluoroborate + water + 1-butanol at 293.15 K, *J. Chem. Eng. Data* **51**, 691–695 (2006).
18. Letcher, T. M., Deenadayalu, N., Soko, B., Ramjugernath, D., and Naicker, P. K., Ternary liquid–liquid equilibria for mixtures of 1-methyl-3-octylimidazolium chloride + an alkanol + an alkane at 298.2 K and 1 bar, *J. Chem. Eng. Data* **48**, 904–907 (2003).
19. Letcher, T. M. and Reddy, P., Ternary liquid–liquid equilibria for mixtures of 1-hexyl-3-methylimidazolium (tetrafluoroborate or hexafluorophosphate) + ethanol + an alkene at T = 298.2 K, *Fluid Phase Equilib*. **219**, 107–112 (2004).
20. Rebelo, L. P. N., Simple g^E-model for generating all basic types of binary liquid–liquid equilibria and their pressure dependence. Thermodynamic constraints at critical loci, *Phys. Chem. Chem. Phys.* **1**, 4277–4286 (1999).
21. Shariati, A. and Peters, C. J., High-pressure phase behavior of systems with ionic liquids: measurements and modeling of the binary system fluoroform + 1-ethyl-3-methylimidazolium hexafluorophosphate, *J. Supercrit. Fluids* **25**, 109–111 (2003).
22. Rebelo, L. P. N., Lopes, J. N. C., Esperança, J. M. S. S., and Filipe, E., On the critical temperature, normal boiling point, and vapor pressure of ionic liquids, *J. Phys. Chem. B* **109**, 6040–6043 (2005).
22. Eckert, F. and Klamt, A., Fast solvent screening via quantum chemistry: COSMO-RS approach, *AIChE J*. **48**, 369–385 (2002).
23. Klamt, A. and Eckert, F., COSMO-RS: a novel and efficient method for the a priori prediction of thermophysical data of fluids, *Fluid Phase Equilib*. **172**, 43–72 (2000). Q3
24. Wu, C.-T., Marsh, K. N., Deev, A. V., and Boxal, J. A., Liquid–liquid equilibria of room-temperature ionic liquids and butan-1-ol, *J. Chem. Eng. Data* **48**, 486–491 (2003).
25. Domańska, U., Pobudkowska, A., and Eckert, F., (Liquid + liquid) phase equilibria of 1-alkyl-3-methylimidazolium methylsulfate with alcohols, or ethers, or ketones, *J. Chem. Thermodyn.* **38**, 685–695 (2006).
26. Klamt, A., Jonas, V., Bürger, T., and Lohrenz, J. C. W., Refinement and parametrisation of COSMO-RS, *J. Phys. Chem. A* **102**, 5074–5085 (1998).
27. Klamt, A. and Schüürmann, G., COSMO—a new approach to dielectric screening in solvents with explicit expressions for the screening energy and its gradient, *J. Chem. Soc. Perkins Trans.* **2**, 799–805 (1993).
28. Eckert, F. and Klamt, A., *COSMOtherm*, Version C2.1, Release 01.05; COSMOlogic GmbH & Co. KG, Leverkusen, Germany, 2005.
29. Eckert, F., *COSMOtherm User's Manual*, Version C2.1, Release 01.05, COSMOlogic GmbH & Co. KG, Leverkusen, Germany, 2005.
30. Schäfer, A., Klamt, A., Sattel, D., Lohrenz, J. C. W., and Eckert, F., COSMO implementation in TURBOMOLE: extension of an efficient quantum chemical code towards liquid systems, *Phys. Chem. Chem. Phys.* **2**, 2187–2193 (2000).
31. This density functional method and basis set combination is equivalent to the Turbomole method. Thus the COSMOtherm parameter set optimized for the Turbomole DFT method can be used with COSMO files produced by this quantum chemical program package.

32. Andzelm, J., Kölmel, C., and Klamt, A., Incorporation of solvent effects into density functional calculations of molecular energies and geometries, *J. Chem. Phys.* **103**, 9312–9320 (1995).

33. Freire, M. G., Carvalho, P. J., Gardas, R. L., Santos, L. M. N. B. F., Marrucho, I. M., and Coutinho, J. A. P., Mutual solubilities of imidazolium-based ionic liquids and water and the Hofmeister series, oral communication presented at EUCHEM Conference on Molten Salts and Ionic Liquids, 2006.

Q4 34. Freire, M. G., Carvalho, P. J., Gardas, R. L., Santos, L. M. N. B. F., Marrucho, I. M., and Coutinho, J. A. P., Mutual solubilities of imidazolium-based ionic liquids and water between (288 and 318) K, *Green Chem.* (submitted).

Author Query

1. OK P?
2. 8.10? OK
3. Pls. check the sequence of references
4. Any update for Ref. 34